Searching for low-energy structures of nanoparticles: a comparison of different methods and algorithms

2009 J. Phys.: Condens. Matter 21 084208

(http://iopscience.iop.org/0953-8984/21/8/084208)

IOP PUBLISHING JOURNAL OF PHYSICS: CONDENSED MATTER

J. Phys.: Condens. Matter **21** (2009) 084208 (11pp) doi:10.1088/0953-8984/21/8/084208

Searching for low-energy structures of nanoparticles: a comparison of different methods and algorithms

G Rossi and R Ferrando

Dipartimento di Fisica, Università di Genova and CNR/INFM, Via Dodecaneso, 33, 16146 Genova, Italy

E-mail: giulia.rossi@fisica.unige.it and ferrando@fisica.unige.it

Received 18 July 2008, in final form 3 September 2008
Published 30 January 2009
Online at stacks.iop.org/JPhysCM/21/084208

Abstract

Nanoparticles can have unusual, low symmetry or non-crystalline shapes. Since structure determines nanoparticle physical and chemical properties, many efforts have been devoted to predict what are the most stable structural motifs depending on cluster size and composition. The global optimization of the $3N$-dimensional potential energy surface of a nanocluster is nevertheless a very difficult computational problem. Here we depict the scenery of the global optimization strategies applied to the study of nanoclusters, focusing on genetic and Basin-hopping approaches. Moreover, several strategies to improve Basin-hopping efficiency are discussed and compared through the optimization of test-systems with different size and composition.

(Some figures in this article are in colour only in the electronic version)

1. Introduction: the global optimization issue in nanocluster science

Global optimization problems have raised alot of interest in the last decades, involving a very broad spectrum of research fields. Logistic problems, like transport managing; computer science problems, like microcircuits or network design; biological problems, like protein folding studies; all of them can be reduced to the same theoretical formulation, namely finding the lowest lying minimum of a given, high-dimensional function $f(\mathbf{X})$. The function to be minimized, from time to time represents the length of the resistive connections in a microchip, or the time requested to drive between two big port cities, or the free energy of a molecule seeking its native configuration. Whatever the problem to be solved, several strategies have been developed to computationally locate, in an as short as possible time, the putative global minimum of f.

The search for the lowest potential energy configuration of an atomic nanocluster is a global optimization problem. One of the key aspects of the study of cluster potential energy surfaces (PES), is the number of local minima—that is, of stable configurations—that lie on the PES. How many are they? How do their numbers increase with cluster size? If it was possible to explore all of them, the global minimum would directly derive from a trivial comparison of the values assumed by f in the local minimum configurations. But unfortunately this is not the case. The number of local minima on the PES of a Lennard-Jones (LJ) cluster with size $N = 100$, according to the last estimates [1], should be larger than 10^{40}. And what is more impressive, it is predicted to increase with cluster size by an exponential function.

In computational complexity theory, problems are classified into P, NP, NP-complete and NP-hard problems (see figure 1), according to the computational resources required to solve them. Details are beyond the scope of the present paper, but we can recall here that the P class consists of all those decision problems (expecting a YES/NO answer) that can be solved by a computer in an amount of time that is polynomial with respect to the size of the input. NP problems consist of all those decision problems whose positive solution can be verified in polynomial time. NP problems are designated as NP-complete if the algorithm used to solved them can also solve all other NP problems. The popular traveling salesman problem belongs to the NP-complete class. Finally, NP-hard problems are the non-decisional version of the NP-complete problems, since a

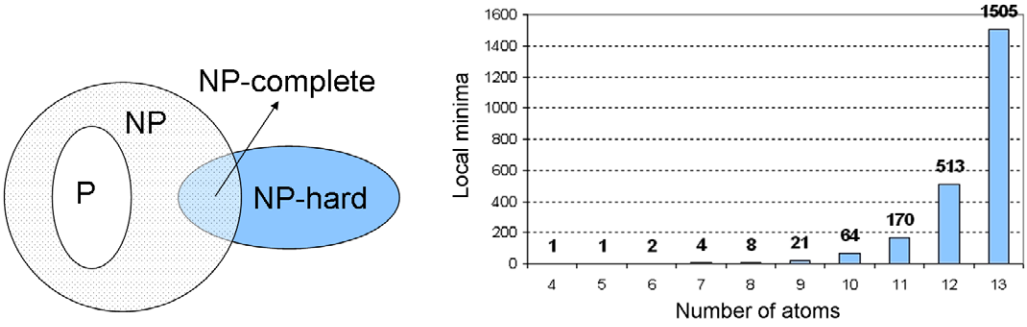

Figure 1. On the left, a schematic representation of P and NP problems. On the right, the exponential growth of the number of local minima on the surface of a Lennard-Jones cluster, as increasing cluster size.

polynomial time algorithm for these problems would solve also the NP-complete problem. In 1985 Wille and Vennik reduced the optimization of the PES of an homogeneous cluster, modeled by a two-body potential, to the non-decisional version of the traveling salesman problem [2], thus demonstrating that the global optimization of cluster PES is an NP-hard problem. Greenwood then generalized [3] the proof to the case of heterogeneous clusters.

The rate of growth of the number of minima lying on the PES depend on the model potential used. As an example, figure 1 shows the increasing of the number of minima versus size in small Lennard-Jones clusters. Quite a simple theory [4–6] suggests that the number of local minima $n_{\min}$ on the PES increases exponentially. If the system is large enough to be divided into m equivalent subsystems of N atoms each, and within the assumption that every subsystem has independent stable configurations, then:

$$n_{\min}(mN) = n_{\min}(N)^m. \tag{1}$$

The equation has thus the exponential solution:

$$n_{\min}(N) = \mathrm{e}^{\alpha N} \tag{2}$$

where α is a system-dependent constant. Moreover, geometrical information still needs to be included in the evaluation of the number of minima lying on the PES. A cluster made up of N atoms has a Hamiltonian that is invariant to (a) all the permutations of atoms of the same species and (b) to the inversion of all coordinates through a space-fixed origin. This means that, given a cluster with a fixed geometrical arrangement, one can think of $N!$ totally equivalent configurations. In other words, each of them is a different point in configuration space corresponding to the same minimum energy value. This number has to be reduced by the order of the symmetry point group of the structure, h.

When dealing with heterogeneous clusters [7], the situation gets more complicated. The presence of two different types of atoms leads to the possibility of *isomers* based on the permutation of unlike atoms, as well as the regular geometrical isomers (with different skeletal structures). Jellinek and Krissinel [8] introduced the term *homotops* to describe A_mB_n alloy cluster isomers, with a fixed number of atoms ($N = m + n$) and composition (m/n ratio), which have the same geometrical arrangement of atoms, but differ in the site labelling, namely the way in which the A and B atoms are arranged. Neglecting symmetry considerations, homotops usually have different potential energies, and an efficient global optimization tool is supposed to explore as large a number as possible of homotops. As the number of homotops increases combinatorially with cluster size, global optimization (in terms of both geometrical isomers and homotops) is an extremely difficult task. Ignoring point group symmetry, a single geometrical isomer of an N-atom cluster, A_mB_n, will give rise to

$$N_{\text{homotops}} = \frac{N!}{n!m!} = \frac{N!}{n!(N-n)!} \tag{3}$$

homotops. For a 20-atom $A_{10}B_{10}$ cluster of a given skeletal structure, for example, there are 184 756 homotops, though many may be symmetrically equivalent.

The paper is structured as follows. In section 2 a quick review of the more common global optimization strategies, namely simulated annealing, genetic and basin-hopping algorithms, is presented. In section 3 we will describe how the performances of the standard basin-hopping algorithm can be improved. Section 4 is devoted to the application of the developed methodologies to the optimization of four test-systems. Finally, conclusions are presented in section 5.

2. Methods for the global optimization of cluster PES

The global optimization of clusters consists in finding, size and chemical composition being fixed, the structural and chemical arrangement of the lowest lying minimum on the PES. With the term *funnel* one usually refers to a funnel-shaped collection of local minima pertaining to the same structural motif. Cluster PESs are often rough and multiple-funnel surfaces. The sampling of minima on such complicate surfaces is a very hard task. Molecular dynamics (MD) approaches are not feasible except for the very small size clusters, since the timescale of an exhaustive exploration of the potential energy surface would definitely exceed the accessible computing timescales of MD. Efforts in the direction of the acceleration of the MD walk have been done in order to reproduce rare events (see, for example, the accelerated MD by Voter [9, 10] applied to the study of metal-on-metal diffusion), nevertheless the pure MD

approach never resulted in a successful optimization strategy. However, since the final goal of global optimization is the location of the lowest lying minimum, MD can be thought as a redundant method to address this aim, including information on the dynamics of the cluster which go beyond the scopes of the search. With a complementary approach, methods based on the totally random generation of cluster configurations have been developed. As an example, we can mention the Big Bang method developed by Jackson [11, 12], who optimized the structure of clusters generating random, highly-compressed configurations of atoms and then relaxing them via a gradient-based algorithm. By iterating the procedure through several millions of searches and shaping the initial compressed configuration according to different aspect-ratios, the authors succeeded in optimizing the structure of $N = 20$–27 Si clusters.

In the following, the most common and effective global optimization methods will be described [13]. Most of them combine elements deriving from a more physical, dynamics-like approach with elements deriving from random sampling. All the algorithms are supposed to run *unbiased* searches, meaning that the starting cluster configuration has random atomic coordinates. Moreover, atoms are not constrained to any lattice position, the discreteness of the three-dimensional space being limited to the computational sensitivity.

2.1. Simulated annealing

In simulated annealing (SA), the system under study is equilibrated at high temperature and then cooled by a Monte Carlo–Metropolis procedure. As the temperature decreases, cluster atoms are progressively frozen in their equilibrium positions. Provided that the temperature decreases logarithmically with time, this leads to the coincidence between free and potential energy minimum [13]. Simulated annealing has two major drawbacks: it is a very time-consuming algorithm, and it can quite easily fail in locating the global minimum configuration of multiple-funnel surfaces. It is possible, indeed, that during cooling the system remains trapped in a free energy minimum that differs from the global minimum of the PES.

Both traditional Newton and Langevin molecular dynamics approaches (see [14] and references therein) have been proposed instead of MC–Metropolis within the simulated annealing scheme. A more recent version of SA has been developed and called conformational simulated annealing (CSA). CSA has been successfully applied both to clusters [15] and biological molecules and proteins [16–18]. In CSA, every point in a configuration space is given the energy of its nearest local minimum by implementing a local minimization procedure. A *bank* of configurations is considered, and subsets of this bank are mutually modified to get new candidate structures. The role of temperature in SA is here played by an order parameter which is used to progressively shrink the area of the configuration space explored.

2.2. Genetic algorithms

Genetic algorithms (GA) have been first proposed by John Holland in the 1970s, and since then they have been used in a variety of fields, including chemistry, physics, economy, computer science, and more. These algorithms are inspired by genetic and evolutionary theories. It is indeed meaningful to refer to populations of individuals (clusters), each one represented by a set of chromosomes (spatial atomic coordinates), living and evolving according to natural selection and adaptability rules. A keyword in this context is *fitness*: it measures how much an individual matches the final requirement, namely having the lowest possible potential energy. In cluster optimization, generation after generation, the individuals that better fit this requirement are selected as parent clusters, in order to preserve the best genetic information and progressively refine the population's characteristics. Natural selection consists indeed in dropping not promising evolutionary branches. Pioneering applications of the genetic strategy to the global optimization of cluster PES were proposed by Hartke [19, 20], who optimized the structure of small Si clusters.

2.2.1. The standard GA design and the SAGA code. After the population initialization, a basic genetic algorithm (see for example the work by Deaven and Ho [21] for an application to fullerene cluster minimization) loops around the following steps:

- fitness evaluation,
- mating,
- mutations,
- acceptance or rejection.

Here we are going to describe the main features of the SAGA algorithm, developed by Rapallo and fruitfully exploited for the optimization of a variety of homogeneous and heterogeneous metallic nanoclusters [22, 23]. A block diagram of SAGA is depicted in figure 2.

Local minimization. The SAGA code implements a L-BFGS local minimization procedure (proposed by Nocedal [24] and based on a quasi-Newton approach). Local minimization is performed upon every new individual generated by mating and mutations, so that only the genetic code corresponding to local minima of the PES becomes available to the next generations.

Speciation into subpopulations. A common problem with the genetic approach is the progressive lack of genetic diversity, which is associated with the concentration of the whole population into the same funnel of the PES. In order to overcome this problem, SAGA code splits up the initial population into several subpopulations, letting them evolve in quite an independent way. The algorithm is thus forced to explore different funnels of the potential energy surface contemporarily. The introduction of subpopulations is of fundamental importance in preserving as long as possible, during evolution, the diversity of the genetic material of the population. The formation of subpopulations is called *speciation* of the original population, and is based on the definition of a geometrical distance between clusters based on Voronoi cells in the $3N$-dimensional space.

The usual configuration of SAGA has $N_{\mathrm{ind}} = 200$ individuals, split into $N_{\mathrm{subpop}} = 5$ subpopulations. During a

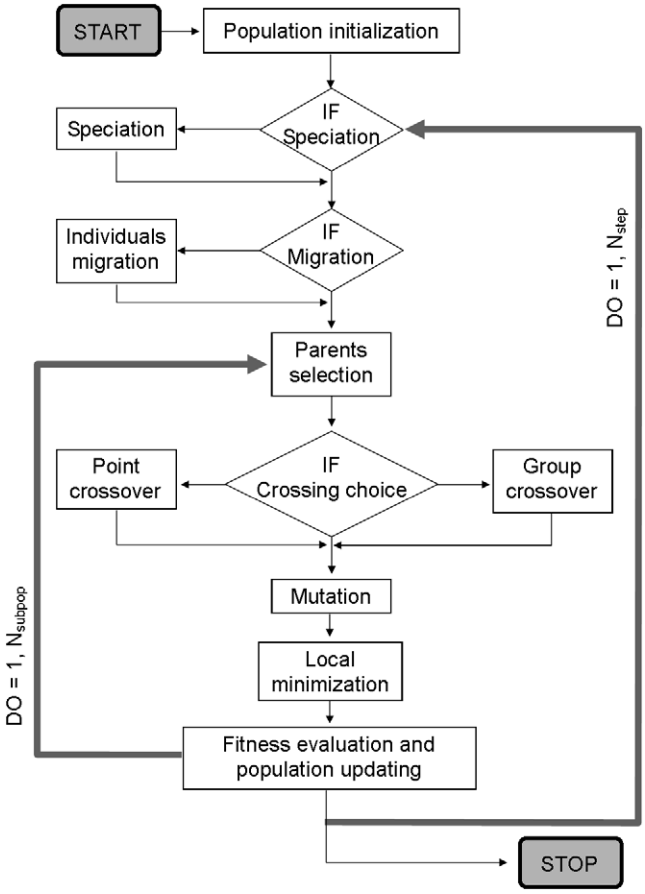

Figure 2. A block diagram of the SAGA code.

single run, clusters can migrate between subpopulations. This *migration* process is regulated by a frequency of migration, so that the transfers of clusters among subpopulations take place all together, and the number of clusters in each subpopulation is constant. The highest fitness clusters are the most likely to be transferred, with the aim of spreading good genetic information. Once the migration process has taken place, evolution continues for a number of generations. Subpopulations are then reformed by speciation.

Mating. Within every subpopulation, a couple of parent individuals generates a pair of new clusters. Parent selection is made according to a *selective pressure*: a high selective pressure means that only the high fitness individuals are likely to be chosen for mating, while a low selective pressure means that also intermediate or poor fitness individuals have some probability to be chosen. For further details about the possible mating strategies, see [25].

Mutations. Several different mutations are applied to the offspring before they are included in the new cluster generation. Some of them involve slight changes in the digits composing cluster chromosomes [25]. As it is expected that the homotops of a heterogeneous cluster have different energies, the exchange mutation has been introduced in the algorithm. This involves exchanging the spatial positions of two atoms of different species in the cluster, and it is applied with a certain probability, for example to every new cluster resulting from the mating process.

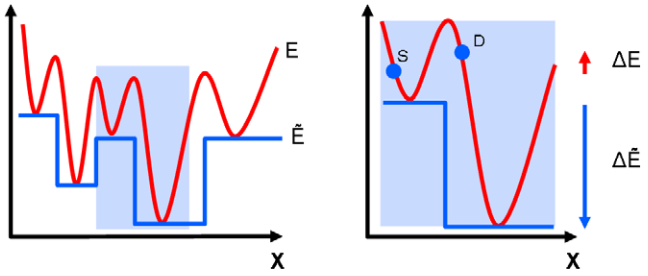

Figure 3. On the left, the PES deformation in BH transforms the original surface in a staircase surface. On the right, zoom in the grey area: if no deformation were applied, the move from S to D could be rejected with probability $1 - e^{(\tilde{E}_S - \tilde{E}_D)/k_B T}$. Thanks to BH local minimization, the acceptability rule compares $\tilde{E}_D$ and $\tilde{E}_S$, thus accepting the move with probability 1.

2.3. Basin-hopping algorithm

Deformation methods alter the shape of the PES by a transformation that reduces the number of local minima or changes their appearance. From a mathematical point of view, such a transformation could change the position and depth of minima, and once located the global minimum of the transformed surfaces, an effective reverse mapping of the surface is required [26]. Basin hopping (BH) belongs to this family, but the local minima of the original PES are exactly reproduced in the transformed surface, so that no reverse mapping is needed. BH has been used to globally optimize a variety of systems, like Lennard-Jones clusters [27–29], molecular clusters, peptides, polymers, and glass-forming solids [26].

The BH transformed landscape is obtained by applying a local minimization procedure to every point in the configuration space:

$$\tilde{E}(\mathbf{X}) = \min\{E(\mathbf{X})\}. \tag{4}$$

In a 2D representation, this would correspond to transforming the energy function into a staircase function, as illustrated in figure 3. During cluster optimization, the sampling of the configuration space is performed by means of a move upon atom coordinates. Moves from a starting configuration, S, to a destination configuration, D, can be accepted or refused according to a standard Metropolis algorithm:

$$\text{if } \tilde{E}_D \leqslant \tilde{E}_S \longrightarrow p = 1 \tag{5}$$

$$\text{if } \tilde{E}_D > \tilde{E}_S \longrightarrow p = e^{-(\tilde{E}_D - \tilde{E}_S)/K_B T} \tag{6}$$

where p indicates the probability of acceptance of the move, and T the fictitious temperature of the system. The importance of the applied transformation appears here quite clearly: as shown in figure 3, if no local minimization was performed, the move from S to D could be rejected even if the $\tilde{E}_D < \tilde{E}_S$ condition was satisfied. In BH algorithm, temperature plays a key role, driving the sampling of configuration space

according to the Boltzmann distribution. BH effectiveness in dealing with multiple-funnel surfaces has also been proved, as in the case of LJ_{38}. This test-bed cluster has a double-funnel PES, with a strict competition between the fcc and the icosahedral (Ih) structural motifs. Wales and co-workers have demonstrated [30, 31, 26] that the transformation of equation (4) causes a broadening of the thermodynamics on the PES, meaning that changes in the global free energy minimum are smoothed on the transformed surface, effectively affecting the occupation probabilities of the different basins in favour of the fcc motif.

In the following, the move strategies implemented in our previous works [25, 22, 23] to select destination configurations are listed.

Moves. During optimization, the candidate destination states are obtained performing a perturbation move upon the starting configurations. In the following, some possible moves are described.

Single move. A single atom is chosen randomly and displaced within a spherical shell centered in its initial position. The new position is chosen accordingly to a uniform spherical distribution. The shell minimum radius is usually fixed to 0, while the maximum one is related to the lattice parameter of the chemical species involved. For the metals considered here, it is usually set equal or slightly lower than half the first neighbour distance.

Shake move. It consists in applying the single move to every atom of the cluster. This is the move that we proved to have the highest efficiency and that we mostly used during the optimization of binary metal clusters.

Ball move. A single atom is displaced to a random position within cluster volume.

Shell move. It is especially designed to get a better arrangement of the cluster surface. A single surface atom is displaced to a random position within a spherical shell roughly corresponding to the external atomic layer of the cluster.

Bond move. This move is designed to act on the weakly bounded atoms. The lowest coordinated atom is displaced according to one of the moves listed above.

Brownian move. Atoms follow very short Langevin dynamics (typically 250 simulation steps, with a time step set to 5 fs) at high temperature. Brownian move proved to be very efficient for the optimization of large clusters ($N > 200$).

High-energy atoms move. A threshold energy is fixed, so that atoms with a lower energy are are displaced according to the shake move, atoms with a higher energy are displaced according to the bond move.

Exchange move. In analogy with what happens in genetic algorithms, exchange moves can also be applied during the optimization of nanoalloy clusters. This move is especially useful when the species in the cluster have the tendency to form mixed bonds. In this class of systems, the configurations differing for an exchange move have quite similar energies, and the optimization of the chemical order has to be led at low temperatures.

2.4. Does memory help to find the global minimum?

All the strategies described up to now have the common characteristic to explore the PES without saving any information about the path followed. The PES is explored relying upon the Boltzmann distribution, a local minimization procedure, and a set of tunable parameters such as the moves probabilities in BH or the mating and mutation operators in GA. Nevertheless, memory would seem to be an integral component of any search that deserves to be called *intelligent*, also from a biological and evolutionary point of view. This idea has been first translated into a global optimization tool with Taboo Search (TS) [32]. According to TS, the optimization code has to retain a memory of the PES regions already visited, so as to avoid falling there again. Taboo regions are indeed the forbidden PES areas.

An alternative way to use memory as a search tool has been proposed by Hansmann and Wille [33]. Their method, called energy landscape paving (ELP), is based on the definition of a histogram function, $H(q,t)$ and of a weight function $f(H(q,t))$, where q is an order parameter and t is a measure of the time elapsed by the beginning of the optimization. The transformed surface upon which the Monte Carlo search takes place is therefore:

$$\tilde{E} = E + f(H(q,t)). \tag{7}$$

The weight of a local minimum state, $p(\tilde{E}) = \mathrm{e}^{-\tilde{E}/k_{\mathrm{B}}T}$, decreases with the time the system stays in that minimum. ELP could be interpreted as a peculiar deformation method, the deformation changing at every step of the optimization. ELP has some similarities with TS, as recently visited regions are not likely to be revisited immediately. Nevertheless, moves towards known funnels are not forbidden, and this could be very important, depending on the connectivity characteristic of the PES. Some *hub* funnel [34] could in fact be connected to several different funnels via different transition states, and TS could in principle allow to explore just one of these escaping path. Within ELP, revisitation moves are given an exponentially lower weight.

Another possible strategy to overcome this problem has been proposed by Goedecker [35]. According to his minima mopping (MH) algorithm, PES is deformed by local minimizations as for BH. The move from a starting state E_{S} to a destination state E_{D} is accepted if the energy of the destination local minimum rises by less than E_{diff} compared to the starting minimum. The parameter E_{diff} is continuously adjusted during simulation so that the rate of acceptance is kept fixed at 50%. What is crucial in MH is the way moves are performed. The idea underlying this procedure is that instead of disfavouring the choice of already visited local minima, it is far more convenient to favour the escaping from such minima. This indeed prevents us from penalizing crossing through important hub funnels. In MH, moves consist in short molecular dynamics simulations. Atoms velocities are initialized according to the value E_{kinetic}, the kinetic energy of the cluster. The escaping from already visited basins is favoured by imposing an high value for E_{kinetic}. This parameter is adjusted dynamically during the simulation, in such a way

that half the number of MD runs lead to never explored minima. As for ELP and TS, MH uses an order parameter to distinguish whether or no a minimum has been already visited.

3. Improving BH performances

Here we are going to discuss some possible strategies to improve the performances of the standard BH algorithm dealing with the PES of heterogeneous nanoclusters.

3.1. Order parameter-based search

In cluster or molecular applications of TS and ELP, the search for the global minimum is driven both in the potential energy and order parameter space, so as to combine energetic and geometric information. The identification of all the competing structural families is an important goal of global optimization approaches based on semi-empirical models, as results can successively be refined by more reliable first-principle energy minimizations.

The choice of the order parameter is a delicate issue. Any prior knowledge about the system under study can be used to get a proper order parameter, nevertheless the search has to preserve its unbiased character. In the following, the order parameters chosen for the optimization of homogeneous and heterogeneous, free and supported clusters are shown.

Common-neighbour analysis. Quite a common instrument for cluster structural characterization is called common-neighbour analysis [36] (CNA). A CNA signature, consisting of three integer numbers (r, s, t), is assigned to each pair of nearest neighbour *nn* atoms A and B. r is the number of common neighbours of A and B, s is the number of *nn* bonds among the r common neighbours, and t is the length of the longest chain that can be formed with the s bonds.

CNA signatures are good candidates as order parameters during global optimizations. Their distribution immediately allows us to distinguish among the well known Ih, decahedral (Dh), and crystalline structural families. Of course, this geometric parameter does not distinguish among chemical ordering, that could play an important role in determining the lowest-energy structural families of heterogeneous clusters. Moreover, depending on the metals considered, signatures to be used as order parameters have to be chosen carefully. In table 1 signature values are reported for the more common structural motifs.

Heterogeneous bonds. Quite a simple way to take into account the cluster chemical arrangement consists in using the number of heterogeneous bonds as an order parameter. Four main types of mixing patterns can be identified for nanoalloys. *Core–shell segregated* nanoalloys consist of a shell of one type of atom (B) surrounding a core of another (A). These clusters will be denoted $A_{core}B_{shell}$. *Sub-cluster segregated* nanoalloys consist of A and B sub-clusters, which may share a large interface with a high degree of mixing, or a smaller neck. *Mixed* A–B nanoalloys may be either ordered or random (i.e a solid solution). *Multishell* nanoalloys may present layered or onion-like alternating ABA shells. A–B bonds are usually maximized by mixed configurations or multishell structures, while perfect $A_{core}B_{shell}$ structures favour the formation of A–A bonds.

Table 1. The percentage of (5, 5, 5), (4, 2, 1) and (4, 2, 2) signatures for Ih, Dh, and TO magic clusters.

N	Structure	(5, 5, 5) %	(4, 2, 1) %	(4, 2, 2) %
13	Ih	28.57	0.00	0.00
19	Double Ih	33.82	0.00	0.00
38	TO	0.00	41.66	0.00
55	Ih	10.3	0.00	38.5
75	Dh	1.25	28.2	20.4
79	TO	0.00	50.0	0.00
147	Ih	5.17	17.24	38.79

Surface contact. During global optimization of metal clusters supported on a surface, other order parameters are required. The number of cluster atoms laying in contact with the oxide surface can be a good order parameter to distinguish between different epitaxies (as the (100) and the (111) epitaxies of the fcc Pd, Ag, Au, Ni, Co clusters [37, 38]).

The order parameter space is not necessarily a one-dimensional space. In the following, one and two order parameters will be used.

3.2. The HISTO algorithm

The Monte Carlo procedure implemented by ELP, as described in section 2.4, does not perform any local minimization. This has proved to be of fundamental importance for BH, GA, and other optimization strategies. We thus developed a new optimization algorithm called HISTO, with local minimizations and all the key features of the memory/order parameter-based searches. HISTO can be considered an improvement of the standard BH procedure, relying on:

- PES transformation into the local minima staircase function,
- sampling of configuration space performed through simple displacements of cluster's atoms,
- an order parameter introducing a memory contribution to the search,
- a method to favour the escape from already visited states and to unfavour the jump into already visited states[1].

HISTO draws a histogram in the order parameter space, normalized to the [0, 1] interval, so as to retain memory of the distribution of the visited states in the order parameter space. In figure 4 an example is shown of a one-dimensional histogram shape modification during the optimization. Here δ indicates the width of histogram bars, while h_i denotes the height of the ith bar. The probability of accepting the move from the minimum E_S to the minimum E_D, is evaluated according to the following rule:

$$p_{SD} = e^{\Delta E^*/k_B T} \qquad \text{where } \Delta E^* = E_D - E_S + w(h_D - h_S). \tag{8}$$

[1] It is also possible to run a version of the HISTO code favouring the escape from already visited funnels in a way which does not depend on the destination state, similarly to what happens in MH. This could actually favour the jumps into *hub* funnels, whose population is crucial in order to access all the remote funnels of the PES.

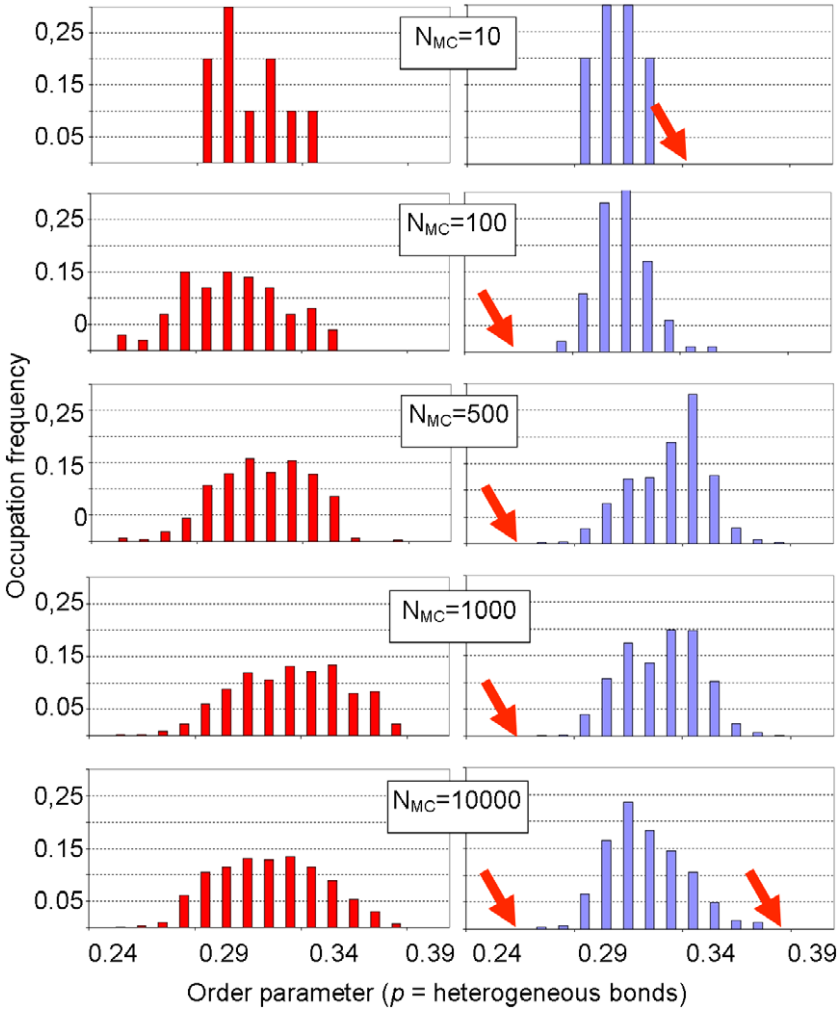

Figure 4. Comparison of a simulation employing the HISTO algorithm (left column) with a standard BH simulation (right column). As the number of Monte Carlo steps increases, the distributions in the order parameter space broaden. In the case of the HISTO simulation, a wider and more homogeneous distribution is obtained. The arrows indicate regions of the order parameter space that are reached by the HISTO simulation but not by the BH simulation, after the same number of Monte Carlo steps.

For $w = 0$, the algorithm reduces to standard BH, while increasing w one gives an increasing weight to the memory contribution.

3.3. Excitable walkers

The second new optimization strategy developed has been called parallel excitable walkers (PEW). The algorithm is described in detail elsewhere [39]. Two walkers k and z, located at the minima $\mathbf{X}_k$ and $\mathbf{X}_z$ are neighbours in a one-dimensional order parameter (p) space if

$$|p(\mathbf{X}_k) - p(\mathbf{X}_z)| \leqslant \delta. \tag{9}$$

The relation can be simply extended to a two-dimensional order parameter space. If a walker laying in its starting position S has at least one neighbour, its transformed potential energy $E_{k\mathrm{S}}$ is substituted by

$$E^*_{k\mathrm{S}} = E_{k\mathrm{S}} + E_{\mathrm{exc}} \tag{10}$$

with $E_{\mathrm{exc}} > 0$. This means that the walker acts as being excited to an energy level placed higher than $E_{k\mathrm{S}}$ by the quantity E_{exc}. PEW reduces to BH for $n_{\mathrm{w}} = 1$. Neighbour walkers have a high probability of accepting energetically unfavourable moves, so that they are likely to increase their distance in the order parameter space. On the other hand, isolated walkers accept mainly energetically favourable moves. In this way, walkers dynamically repel each other, but their mobility is not hindered by a static repulsion term, so that they can move efficiently across distinct regions of the order parameter space, which are possibly related to different funnels. Since interfunnel moves are possible thanks to the excitation energy E_{exc}, the PEW algorithm can be used at very low temperatures, thus being very efficient also in reaching the bottom of a given funnel.

4. Results

In the following, the performances of the two new BH-based algorithms, namely HISTO and PEW, are compared to

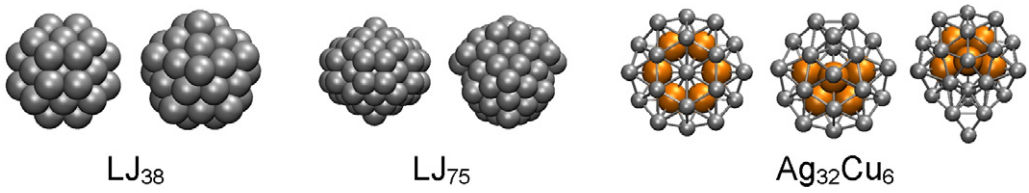

Figure 5. Global minima (left) and competing minima (right) for the three gas-phase systems treated in the text. In $Ag_{32}Cu_6$, external Ag atoms are represented by the small spheres, whereas inner Cu atoms are represented by the large spheres. Two competing minima are shown for $Ag_{32}Cu_6$. The last one has exactly the same $p_{(5,5,5)}$ as the global minimum.

standard BH performances. Two Lennard-Jones homogeneous clusters, LJ_{38} and LJ_{75}, and two heterogeneous metallic cluster, $Ag_{32}Cu_6$ and $Au_{90}Cu_{90}$, have been chosen as test-systems (see figure 5). Shake move is adopted by all the algorithms. Algorithms start from a random configuration and run $N_{MC} = 10^6$ MC steps, each one corresponding to an attempted move, namely to a local minimization. The time requested by the local minimization is almost 100% of cpu time spent at each step. In the PEW case, it is worth noting that the number of MC steps per walker is N_{MC}/n_w. Each time the (known) global minimum is found, the simulation is restarted from a random configuration. N_s denotes the number of times the global minimum has been found within 10^6 MC steps.

LJ_{38}

Lennard-Jones potential has been implemented with the parameters of argon, $\epsilon = 119$ K and $\sigma = 3.4$ Å. Both in PEW and HISTO runs, the percental occurrence of the (5, 5, 5) CNA signature, $p_{(5,5,5)}$, is used as an order parameter. The global minimum of LJ_{38} is an fcc truncated octahedron (see figure 5), for which $p_{(5,5,5)} = 0$. This cluster lies at the bottom of a deep, narrow funnel, and it is in competition with structures pertaining to a five-fold symmetry funnel. The best minimum belonging to this funnel is the slightly distorted decahedron shown in figure 5, whose order parameter value is $p_{(5,5,5)} = 8.16\%$.

The results of the optimizations of LJ_{38} are reported in figure 6. The BH algorithm is mostly effective in the range 100–300 K, where it obtains a number of successful optimizations $N_s \approx 400$, which means an average of 2500 MC steps to reach the global minimum. To make a comparison of our BH with the BH results shown by Wales and Doye [28], we have calculated the frequency of successful optimizations within 5000 MC steps, and found a percentage close to 90%. According to Wales and Doye [28], 4 over 5 runs of 5000 MC steps were able to find the global minimum of LJ_{38}.

The PEW algorithm is mostly effective at low temperatures, in the range 10–50 K. PEW performances are described in detail in [39]. The fraction of successful optimizations that locates the GM within 5000 MC steps is of more than 99% (to be compared also to the 96% of the basin-hopping occasional jumping algorithm [40]). At its best performance, the PEW algorithm visits a very small average number of minima (≈300) before reaching the global minimum. This number is even lower than for the minima Hopping algorithm [35], for which the best performance is 410.

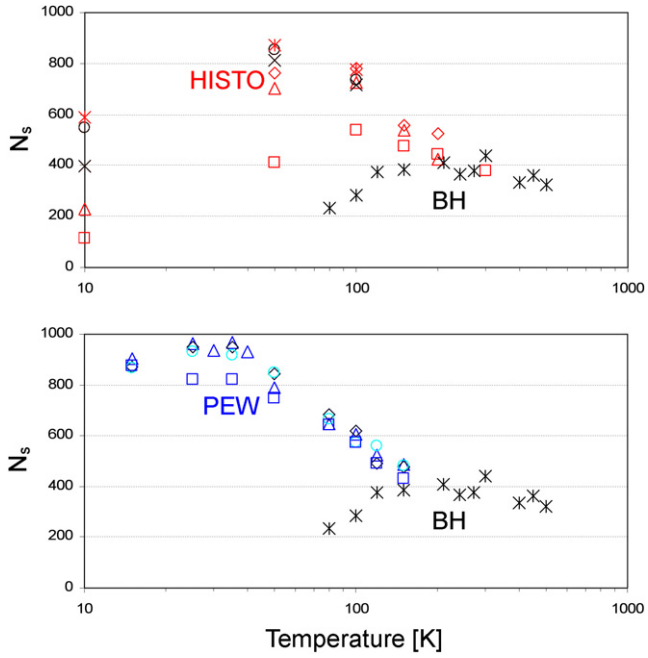

Figure 6. Results of the optimizations of LJ_{38}. Temperature, on the x axis, is plotted on a logarithmic scale. Black stars, repeated in both the graphs, refer to BH algorithm. On top, the comparison between HISTO and BH performances. Open squares refer to a weight $w = 0.1$ eV, triangles to $w = 0.3$ eV and circles to $w = 0.5$ eV. The HISTO efficiency is improved if the histogram is periodically reset during optimization. Open stars, full circles and open crosses correspond to a weight $w = 0.5$ eV, with histograms reset respectively every 5×10^4, 10^4 and 5×10^3 MC steps. Results related to 10^4 step-resetting are averaged over four optimization runs. On the bottom are the comparison between PEW and BH performances. The best BH performances are placed in the temperature range 100–300 K, while PEW best results are obtained below 100 K. Open rhombi, triangles and circles refer to PEW algorithm with $n_w = 3$, $\delta = 0.02$ and $E_{exc} = 0.04$, 0.06 and 0.08 respectively. Open squares correspond to $n_w = 4$, $\delta = 0.015$ and $E_{exc} = 0.06$.

The best HISTO performances are placed in an intermediate temperature range, 50–100 K. The number of successes is competing with that by the PEW algorithm, though slightly smaller. Results indicate that the HISTO code is able to locate the global minimum more than 700 times every million steps, that is about every 1400 MC steps. Results are improved if during the optimization run the histogram is periodically reset. This is somehow predictable, because HISTO code is just designed in order to subvert the occupation probabilities induced by the thermodynamic of the system, and finally leads

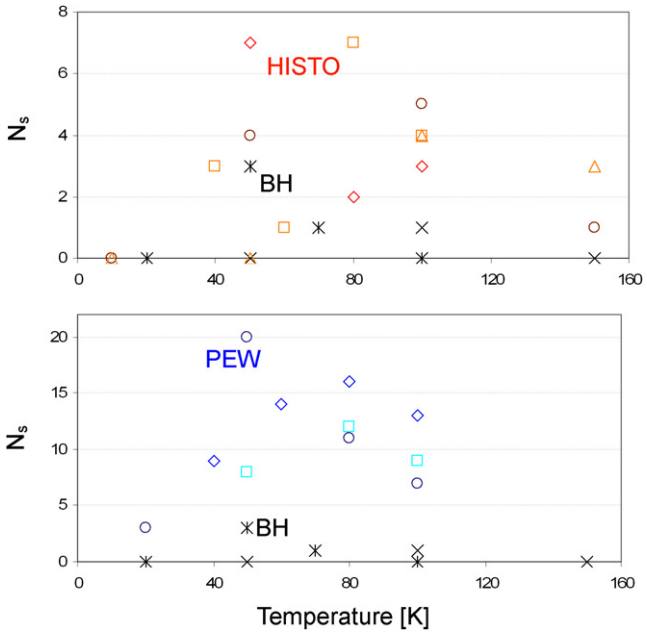

Figure 7. On the top the comparison between HISTO and BH. Black crosses and stars refer to standard BH, respectively to a single 10^6 MC steps run and 200 runs of 5×10^3 MC steps. On top, BH is compared to HISTO algorithm. Standard HISTO is represented by open circles and rhombi. HISTO with resetting of the histogram every 10^4 steps is represented by open triangles. Open squares represent HISTO with the double $p_{(4,2,2)}$ and $p_{(5,5,5)}$ order parameter. On the bottom, BH is compared to PEW algorithm. Open squares represent PEW in the double order parameter space. Open rhombi and circles refer to PEW with the single order parameters.

us to draw a uniform distribution of minima in the order parameter space.

LJ_{75}

In this case, the global minimum is a Marks truncated decahedron [41] (see figure 5), competing with icosahedral structures which are at the bottom of a much wider funnel. Data about the optimization of LJ_{75} are collected in figure 7. In several runs (10^6 MC steps) at different temperatures, the global minimum has been reached by BH only once. The difficulty of BH to get into the right funnel from a random configuration was already pointed out by Wales and Doye [28]. In order to overcome this difficulty, we run 200 short simulations (5000 MC steps) starting from different random configurations, so that some of them can hopefully start in the decahedral funnel. In this way the global minimum is found more easily, up to three times at temperature $T = 50$ K.

The PEW algorithm ($p_{(5,5,5)}$ order parameter) performs much better, counting ≈15 successful searches within 10^6 MC steps. Another possible strategy to help the exploration of the decahedral funnel during the search consists in changing the order parameter from $p_{(5,5,5)}$ to $p_{(4,2,2)}$. The (4, 2, 2) signature is typical of the pairs of atoms placed at interfaces between tetrahedra in both Ih and Dh structures. The (4, 2, 2) signature is indeed absent in TO clusters, and present, but with very different percentages, in decahedra and icosahedra. PEW simulations using $p_{(4,2,2)}$ have been indeed able to locate the global minimum structure up to 20 times within a million MC steps, which is the best result collected so far.

Concerning HISTO performances, both resetting and not resetting histogram codes have been used, and both single ($p_{(5,5,5)}$) and double ($p_{(4,2,2)}$ and $p_{(5,5,5)}$) order parameters have been tested. Standard HISTO with a weight $w = 0.5$ and $p_{(5,5,5)}$ gets a number of successes that is only slightly better than BH (global minimum is found 4 or 5 times in one million steps, in the temperature range 50–100 K), and the same happens also resetting the histogram every 10^4 steps. Increasing the weight to $w = 0.7$ leads to the result $N_s = 7$ for $T = 50$ K. Using the double $p_{(4,2,2)}$ and $p_{(5,5,5)}$ order parameter, and a weight $w = 0.7$, the higher number of successes is again $N_s = 7$.

$Ag_{32}Cu_6$

According to our model potential the global minimum of $Ag_{32}Cu_6$ is the six-fold pancake (see figure 5), a polyicosahedral cluster of symmetry group D_{6h} in which the Cu atoms form a non-compact inner hexagonal ring. The ratio between the number of mixed Ag–Cu *nn* bonds and the total number of *nn* bonds is chosen as order parameter, denoted by p_{mb}. p_{mb} is able to discriminate between core–shell and alloyed structures, and also to discriminate between core–shell structures having either a compact or a non-compact Cu core. At the chemical composition considered here, p_{mb} takes values in the interval [0.2, 0.4]. The global minimum is at the bottom of a narrow funnel, and has a large number of mixed bonds, with $p_{mb} = 0.38$. The competing structures in figure 5 have compact Cu cores and $p_{mb} = 0.31$, being thus well separated from the global minimum in the order parameter space. The results are shown in figure 8, where BH, PEW and HISTO algorithms are compared.

BH is mostly effective in the range 1000–2000 K, while the best performance of PEW is from 100 to 800 K. Very good results are obtained for wide ranges of parameters, $2 \leqslant n_w \leqslant 8$, and $E_{exc} = 0.4$ eV. Comparing the best performances of PEW and BH, we see that the former is about 3.5 times faster.

For $Ag_{32}Cu_6$ optimization, the best performances have been obtained by the HISTO code. Resetting the histogram every 10^4 and 5×10^3 steps, it has been able to locate the global minimum structure up to 187 times in one million steps, that means that, on the average, 5348 local minimizations are needed before finding the $Ag_{32}Cu_6$. It is worth noting here that the performances of HISTO code, with the reset option switched on, are suddenly dumped as temperature is increased beyond 1000 K. The exploration of a wider portion of the PES due to the higher temperature which indeed contrasts the filling of histogram bars, and it can be expected that at higher temperatures results could be improved by a longer reset time.

Large heterogeneous clusters

The global optimization of large heterogeneous clusters ($N >$ 100 atoms) is a very hard task. Nevertheless, global optimization approaches can be useful in identifying all the

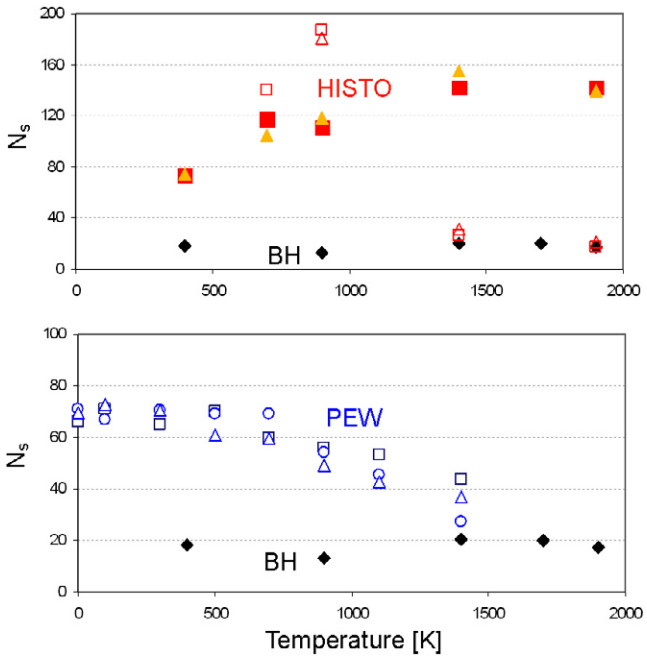

Figure 8. Results of the optimization of $Ag_{32}Cu_6$. Full black rhombi, repeated in both the graphs, refer to BH optimizations. At the top, the comparison between HISTO and BH performances. Full squares and triangles refers respectively to weights $w = 6.0$ and 5.0 eV. As in LJ_{38} case, HISTO performances can be improved if the histogram is periodically reset. Open squares and triangles refer respectively to HISTO with $w = 6.0$ eV and histogram resetting every 10^4 and 5×10^3 steps. At the bottom, the comparison between PEW and BH performances. Squares refer to PEW with $n_w = 5$, $\delta = 0.02$, $E_{exc} = 0.5$. Triangles refer to PEW with $n_w = 3$, $\delta = 0.02$, $E_{exc} = 0.7$, while circles correspond to $n_w = 3$, $\delta = 0.02$, $E_{exc} = 0.5$.

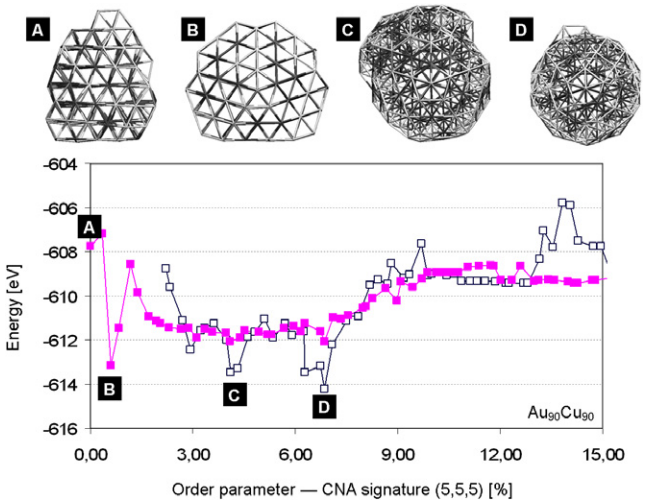

Figure 9. The best minima collected by two PEW optimization runs for the $Au_{90}Cu_{90}$ cluster.

competing structural families, providing candidates whose chemical order and structure can be further refined by seeded optimization runs. The algorithms we described so far are able to deal with cluster sizes up to 500 atoms. The use of structural order parameters allows us to locate and classify the structural motifs corresponding to low-energy values on the PES. Here we report about the optimization of a $Au_{90}Cu_{90}$ cluster by the PEW algorithm. The order parameter chosen for both the optimization runs is the (5, 5, 5) CNA signature. 4 and 8 walkers are employed, with $E_{exc} = 0.5$ eV. During the optimization runs, minima are classified according to the value or the order parameter and collected, as shown in figure 9. The PES of the cluster contains at least four different funnels: (a) the fcc funnel (corresponding to $p_{(5,5,5)} = 0$, as no local five-fold symmetries are present in the skeletal structure of the cluster) (b) the decahedral funnel ($0.5 < p_{(5,5,5)} < 1$) (c) the Mackay icosahedral funnel (the best structure located within this funnel is a perfect 147-atom plus a Mackay shell) and (d) the anti-Mackay funnel. The PEW optimization approach is thus able to locate several competing funnels on the PES of a large heterogeneous cluster.

Finally, the best configuration within each structural motif can be further refined from the point of view of the pure chemical ordering. As we mentioned at section 2.3, the exchange move is especially effective in systems where the two metal species have some tendency to mix. This is the case for Au and Cu, which present three alloy stoichiometries in the bulk and only a slight tendency of Au to the segregation at the surface of Cu. Once the best candidates within each funnel of the PES are located by the global optimization approach, they are used as seeds for some thousand steps of optimization using the exchange move only, at low temperature. This allows us to refine the chemical order of the cluster, obtaining results which are by far more satisfying than those obtained by running the exchange and the shake (or Brownian) move during the unseeded optimization. The reasons for this failure can be explained as follows. When running low-T PEW optimizations, the use of the exchange move allows a very fast convergence to the lowest lying minima of the starting funnel, thus making it more and more difficult to escape from it.

5. Conclusions

In this paper we outlined the scenery of the global optimization of the potential energy surface of nanoclusters, both homogeneous and heterogeneous. Several computational approaches to the problem were analysed, ranging from GA to BH-like approaches. Two algorithms, PEW and HISTO, both based on a BH architecture, were used for global optimization of four test-systems and their performances were compared to the BH performances. Both the algorithms were able to locate the global minimum configuration of the test clusters up to eight times more than the standard BH. Finally, some general trends for the choice of the appropriate temperatures, order parameters and move schemes are offered so as to be able to effectively optimize the PES of different nanoparticles.

References

[1] Leary R H 2000 *J. Global Opt.* **18** 367
[2] Wille L T and Vennik J 1985 *J. Phys. A: Math. Gen.* **18** L419
[3] Greenwood G W 1999 *Int. J. Res. Phys. Chem. Chem. Phys.* **211** 105

[4] Stillinger F H and Weber T A 1982 *Phys. Rev.* A **25** 978
[5] Stillinger F H and Weber T A 1984 *Science* **225** 983
[6] Stillinger F H 1999 *Phys. Rev.* E **59** 48
[7] Ferrando R, Jellinek J and Johnston R L 2008 *Chem. Rev.* **108** 845
[8] Jellinek J and Krissinel E B 1999 *Theory of Atomic and Molecular Clusters* (Berlin: Springer)
[9] Voter A F 1999 *J. Chem. Phys.* **106** 4665
[10] Voter A F, Montalenti F and Germann T C 2002 *Annu. Rev. Mater. Res.* **32** 321
[11] Jackson K A, Horoi M, Chauduri I, Frauenheim T and Schvartsburg A A 2004 *Phys. Rev. Lett.* **93** 013401
[12] Jackson K A, Horoi M, Chauduri I, Frauenheim T and Schvartsburg A A 2006 *Comput. Mater. Sci.* **35** 232
[13] Wales D J and Sheraga H A 1999 *Science* **285** 1368
[14] Binggeli N, Martins J L and Chelikowsky J R 1992 Simulations of si clusters via langevin molecular dynamics with quantum forces *Phys. Rev. Lett.* **68** 2956
[15] Lee I-H, Lee J and Lee J 2003 *Phys. Rev. Lett.* **91** 080201
[16] Lee J, Sheraga H A and Rackovsky S 1997 *J. Comput. Chem.* **18** 1222
[17] Lee J K and Sheraga H A 1999 *Int. J. Quantum. Chem.* **75** 255
[18] Kim S Y, Lee S B and Lee J 2005 *Phys. Rev.* E **72** 011916
[19] Hartke B 1993 *J. Phys. Chem.* **97** 9973
[20] Hartke B 1995 *Chem. Phys. Lett.* **240** 560
[21] Deaven D M and Ho K M 1995 Molecular geometry optimization with a genetic algorithm *Phys. Rev. Lett.* **75** 288
[22] Rapallo A, Rossi G, Ferrando R, Fortunelli A, Curley B C, Lloyd L D, Tarbuck G M and Johnston R L 2005 *J. Chem. Phys.* **122** 194308
[23] Rossi G, Rapallo A, Mottet C, Fortunelli A, Baletto F and Ferrando R 2004 *Phys. Rev. Lett.* **93** 105503
[24] Nocedal J 1980 *Math. Comput.* **35** 773
[25] Rossi G, Ferrando R, Rapallo A, Fortunelli A, Curley B C, Lloyd L D and Johnston R L 2005 *J. Chem. Phys.* **122** 194309
[26] Wales D J 2003 *Energy Landscapes with Applications to Clusters, Biomolecules and Glasses* (Cambridge: Cambridge University Press)
[27] Wales D J, Doye J P K, Dullweber A, Hodges M P, Naumkin F Y, Calvo F, Hernndez-Rojas J and Middleton T F *The Cambridge Cluster Database* http://www-wales.ch.cam.ac.uk/CCD.html
[28] Wales D J and Doye J P K 1998 *J. Phys. Chem.* A **101** 5111
[29] Leary R H and Doye J P K 1999 *Phys. Rev.* E **60** R6320
[30] Doye J P K and Wales D J 1998 *Phys. Rev. Lett.* **80** 1357
[31] Doye J P K, Wales D J and Miller M A 1998 *J. Chem. Phys.* **109** 8143
[32] Glover F 1989 *ORSA J. Comput.* **1** 190
[33] Hansmann U H E and Wille L T 2002 *Phys. Rev. Lett.* **88** 068105
[34] Doye J P K and Massen C P 2005 *J. Chem. Phys.* **122** 084105
[35] Goedecker S 2004 *J. Chem. Phys.* **120** 9911
[36] Faken D and Jonsson H 1994 *Comput. Mater. Sci.* **2** 279
[37] Rossi G, Mottet C, Nita F and Ferrando R 2006 *J. Phys. Chem.* B **110** 7436
[38] Ferrando R, Rossi G, Nita F, Barcaro G and Fortunelli A 2008 *ACS Nano* **2** 1849
[39] Rossi G and Ferrando R 2006 *Chem. Phys. Lett.* **423** 17
[40] Iwamatsu M and Okabe Y 2004 *Chem. Phys. Lett.* **399** 396
[41] Baletto F and Ferrando R 2005 *Rev. Mod. Phys.* **77** 371